Volume Title
ASP Conference Series, Vol. **Volume Number**
Author

New Observational Evidence of Flash Mixing on the White Dwarf Cooling Curve

T.M. Brown,[1] T. Lanz,[2] A.V. Sweigart,[3] Misty Cracraft,[1] Ivan Hubeny,[4] and W.B. Landsman[5]

[1]*Space Telescope Science Institute, 3700 San Martin Drive, Baltimore, MD 21218*

[2]*Department of Astronomy, University of Maryland, College Park, MD 20742*

[3]*Code 667, NASA Goddard Space Flight Center, Greenbelt, MD 20771*

[4]*Steward Observatory, University of Arizona, Tucson, AZ 85712*

[5]*Adnet Systems, NASA Goddard Space Flight Center, Greenbelt, MD 20771*

Abstract.
Blue hook stars are a class of subluminous extreme horizontal branch stars that were discovered in UV images of the massive globular clusters ω Cen and NGC 2808. These stars occupy a region of the HR diagram that is unexplained by canonical stellar evolution theory. Using new theoretical evolutionary and atmospheric models, we have shown that the blue hook stars are very likely the progeny of stars that undergo extensive internal mixing during a late helium-core flash on the white dwarf cooling curve. This "flash mixing" produces hotter-than-normal EHB stars with atmospheres significantly enhanced in helium and carbon. The larger bolometric correction, combined with the decrease in hydrogen opacity, makes these stars appear subluminous in the optical and UV. Flash mixing is more likely to occur in stars born with a high helium abundance, due to their lower mass at the main sequence turnoff. For this reason, the phenomenon is more common in those massive globular clusters that show evidence for secondary populations enhanced in helium. However, a high helium abundance does not, by itself, explain the presence of blue hook stars in massive globular clusters. Here, we present new observational evidence for flash mixing, using recent *HST* observations. These include UV color-magnitude diagrams of six massive globular clusters and far-UV spectroscopy of hot subdwarfs in one of these clusters (NGC 2808).

1. Introduction

In an old stellar population of a given age and chemical composition, the horizontal branch (HB) is the locus of stars undergoing stable helium burning in the core, where the extent in effective temperature arises from a range of envelope mass. In globular clusters hosting extreme HB (EHB) stars at temperatures $T_{\rm eff} \gtrsim 16,000$ K, the hot end of the HB appears nearly vertical in optical color-magnitude diagrams (CMDs), due to a color degeneracy with temperature as the stellar luminosity shifts from optical to ultraviolet wavelengths. However, UV photometry of ω Cen demonstrated that it hosts a population of subluminous EHB stars that form a "blue hook" (BH) at the hot end of the canonical EHB (D'Cruz et al. 1996, 2000). D'Cruz et al. (1996) proposed that such

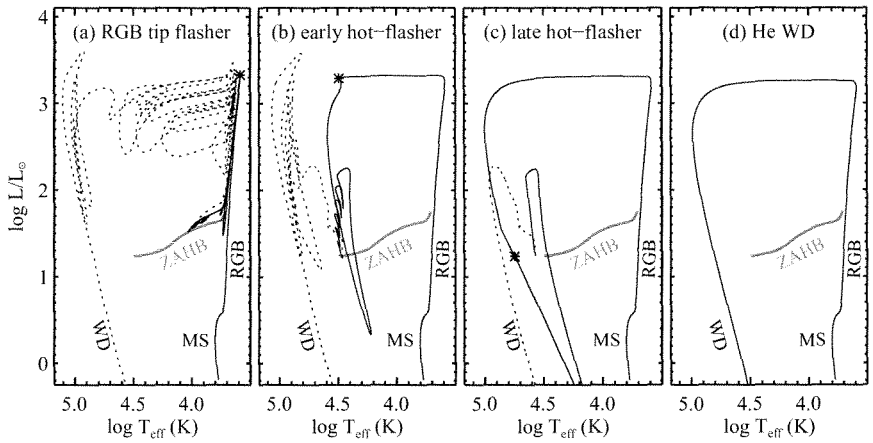

Figure 1. Various evolutionary paths for producing an HB star (from Brown et al. 2010). The zero-age HB (ZAHB) phase is highlighted in grey, while the pre-ZAHB evolution (solid curves) and post-ZAHB evolution (dashed curves) are in black. The peak of the helium-core flash is marked by an asterisk. The four panels show the evolution for progressively larger amounts of mass loss on the RGB. The evolution in the first two panels produces canonical HB stars in which the H-rich surface composition does not change during the helium-core flash. In the third panel, the helium-core flash occurs on the WD cooling curve, producing a flash-mixed star having a surface composition highly enriched in helium and carbon and a temperature significantly hotter than the canonical HB. In the fourth panel, the helium flash never occurs and the star dies as a helium WD.

stars may have undergone a delayed helium-core flash after peeling away from the red giant branch (RGB) due to high mass loss.

We now know that stars can follow a variety of evolutionary paths to the HB, depending on when the helium-core flash occurs (see Figure 1). For normal rates of mass loss, the helium-core flash will occur at the RGB tip (RGB tip flasher, Figure 1a). However, for sufficiently high rates of mass loss, the helium-core flash can occur either during the crossing of the HR diagram (early hot flasher, Figure 1b) or on the white dwarf (WD) cooling curve (late hot flasher, Figure 1c), as first shown by Castellani & Castellani (1993). Brown et al. (2001) demonstrated that a delayed helium-core flash on the WD cooling curve would result in a stellar atmosphere extremely enhanced in helium (~96% by mass), with significant enhancements of carbon and/or nitrogen (~1 to 4% by mass), due to the mixing of the stellar envelope into the hot helium-burning core. This "flash mixing" decreases the opacity below the Lyman limit, thereby lowering the flux at longer wavelengths, and increases the effective temperature in the EHB stars, thereby increasing the bolometric correction. Brown et al. (2001) found that both of these effects together might explain the BH feature in the UV CMD of NGC 2808. Evidence for BH populations in other clusters soon followed, including NGC 6715 (Rosenberg, Recio-Blanco, & García-Marín 2004), NGC 6388 (Busso et al. 2007), NGC 2419 (Ripepi et al. 2007), NGC 6273 (noted by Rosenberg, Recio-Blanco, & García-Marín 2004; Piotto et al. 1999, first appearance), and NGC 6441 (Busso et al. 2007; Dieball et al. 2009).

Here we present observational evidence for the flash-mixing mechanism in those EHB stars that are subluminous with respect to the expectations from canonical stellar evolution theory. This evidence includes new observations from the *Hubble Space Telescope (HST)*. We will examine far-UV and near-UV photometry of massive globular clusters spanning a wide range of metallicity, and far-UV spectroscopy of both normal and subluminous EHB stars in one of these clusters (NGC 2808).

2. Imaging

We have obtained far-UV and near-UV photometry of six massive globular clusters (Brown et al. 2001, 2010). The far-UV images were obtained using the Space Telescope Imaging Spectrograph (STIS) and the Solar Blind Channel on the Advanced Camera for Surveys (ACS). The near-UV images were obtained using STIS, the Wide Field and Planetary Camera 2, and the High Resolution Camera on ACS. Although the bandpasses employed vary from cluster to cluster, the distinctions are not large enough to hamper comparisons of the resulting CMDs, and are in any case included in our transformations of models to the observational plane (for details, see Brown et al. 2010).

The CMD for each cluster is shown in Figure 2. Each cluster exhibits a distinct hook feature at the hot end of its HB locus. As discussed extensively in Brown et al. (2001), this hook feature cannot be due to photometric scatter, differential reddening, or instrumental effects, because these mechanisms could not affect the photometry of the EHB without also affecting the photometry of the HB stars lying immediately to the red of the EHB. The EHB stars span a much larger luminosity range, despite their similar far-UV luminosities and photometric errors.

We compare our CMDs to stellar evolutionary models by transforming these models to the observational plane using self-consistent non-LTE model atmospheres and synthetic spectra (Brown et al. 2010). We begin with canonical evolutionary models at standard helium abundance ($Y = 0.23$; Figure 2). We adopt metallicity and distance values that are representative of values in the literature, and then make small adjustments to the extinction so as to place the blue HB stars ($7000 \lesssim T_{\rm eff} \lesssim 15,000$ K) in the model at the expected location. For the four metal-poor clusters, the theoretical HB distribution should be coincident with the observed HB locus at these intermediate temperatures. For the two metal-rich clusters, however, Rich et al. (1997) have shown that the HB slopes strongly upward as one moves from the reddest HB stars to the top of the blue HB tail (see also Busso et al. 2007), such that the blue HB is ~0.5 mag brighter than one would expect for a canonical locus normalized to the red HB. This increase in HB luminosity at hotter temperatures is what one would expect if the hotter HB stars were preferentially drawn from populations increasing in helium abundance, up to $Y \sim 0.4$ on the EHB. For this reason, we normalize the canonical HB locus for these two clusters (Figure 2) to a point 0.5 mag fainter than the observed blue HB. Of course, it would be simpler to consistently align our models to the red HB in all of our clusters, but it falls outside of our UV CMDs, thus requiring us to use the blue HB.

Next, in Figure 3, we compare our photometry to the expectations from evolutionary tracks with enhanced helium ($Y = 0.4$), assuming the same cluster parameters (reddening and distance) as for the standard Y tracks. At first glance, an enhanced helium abundance offers a promising solution to the BH puzzle, because HB models with enhanced helium exhibit a sharp downturn at the hot end of the HB, reminiscent of the BH feature. However, the downturn in such a model arises from the combination of two

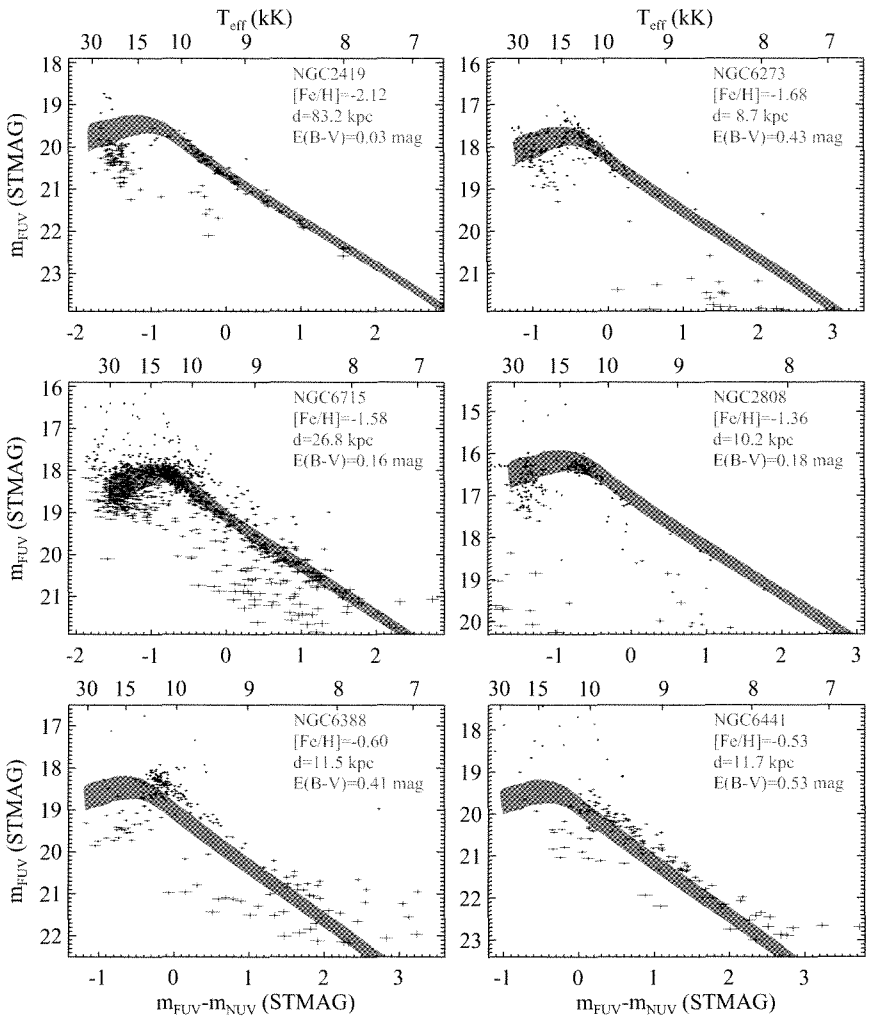

Figure 2. Ultraviolet CMDs for six massive globular clusters spanning a wide range in [Fe/H] (points), along with the HB locus expected from canonical stellar evolution theory at standard helium abundance (Y = 0.23; violet shaded area). The assumed cluster parameters are indicated (grey labels). An approximate conversion (assuming normal cluster abundances) between observed color and effective temperature is shown on the upper abscissa in each panel. Photometric errors (blue bars) are only significant for stars much redder and fainter than the EHB stars that are the focus of this paper. The BH population appears as a downward hook at the hot end of the observed HB, where it deviates below the canonical EHB. For the two metal-rich clusters, that deviation occurs far to the red of the hot end of the canonical HB.

effects: a relatively small decrease in luminosity on the hot end of the HB, and a significant increase in luminosity at cooler temperatures (compare violet and green models in Figure 3). As is evident in Figure 3, the locus of the Y = 0.4 models is much brighter

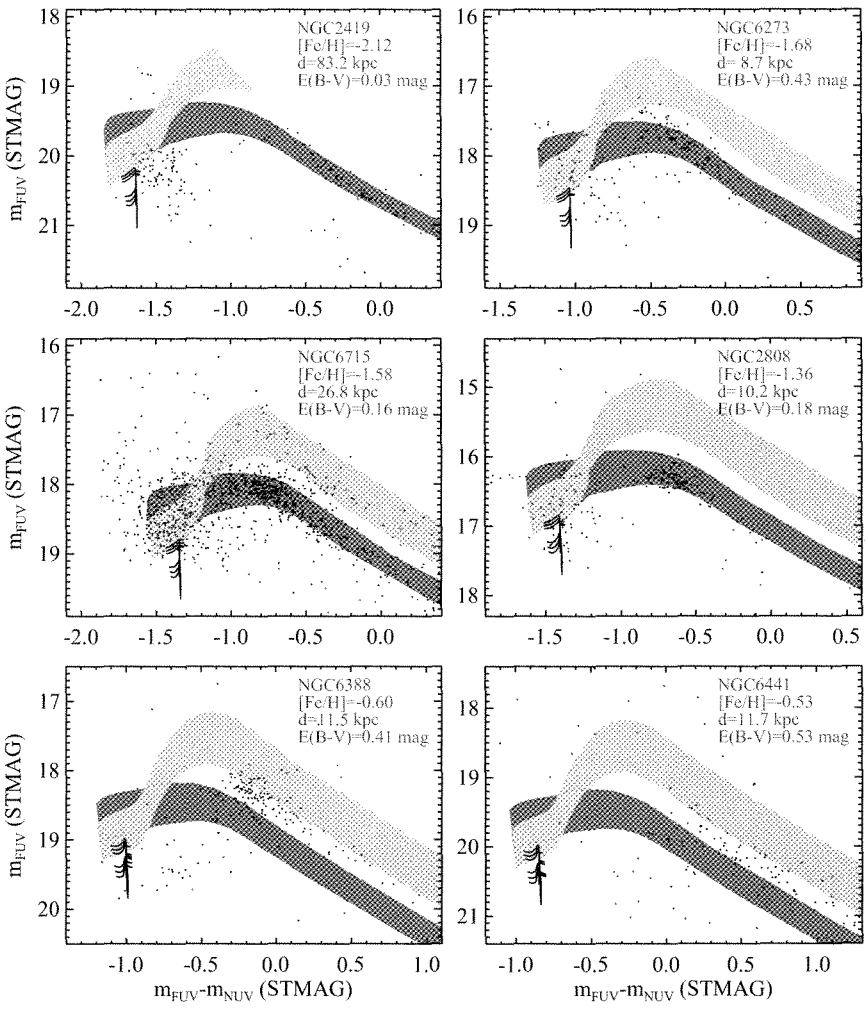

Figure 3. Our UV CMDs compared to canonical models at standard helium abundance ($Y = 0.23$; violet), canonical models at enhanced helium abundance ($Y = 0.4$; green), and flash-mixed models for stars born at standard helium abundance (blue curves) and enhanced helium abundance (brown curves). The combination of canonical and flash-mixed models is able to reproduce the full luminosity width of the observed EHB, but not the red colors seen in some of the BH stars.

than the blue HB population in all of the clusters. For this reason, a $Y = 0.4$ HB model cannot, by itself, explain the observed luminosity difference between the blue HB and BH stars. However, because it is easier to produce EHB stars in a helium-enriched population, the HB population in each cluster may host EHB stars preferentially drawn from that subset of the cluster population enhanced in helium. The existence of helium-enhanced subpopulations in massive globular clusters, including NGC 2808 (D'Antona et al. 2005; Piotto et al. 2007) and NGC 6715 (Layden & Sarajedini 2000; Siegel et

al. 2007) is the leading explanation for the splitting of the main sequence and subgiant branch recently discovered in optical CMDs of these clusters. In those clusters exhibiting multiple main sequences, the bluer main sequence is attributed to a higher helium abundance up to $Y \sim 0.4$ (Piotto et al. 2005); in ω Cen, the bluer main sequence is actually more metal rich.

Finally, we compare our CMDs to models for stars that underwent a late helium-core flash on the white dwarf cooling curve (Figure 3). We show such models for stars born on the main sequence with both standard helium abundance ($Y = 0.23$; blue curves) and enhanced helium abundance ($Y = 0.4$; brown curves). Instead of plotting the core helium-burning locus of all BH stars, we show three representative tracks in each category; two of these tracks fall at the extremes of the range in the mass loss rate leading to flash mixing, while one falls halfway between these extremes. Although the range of mass loss that leads to flash mixing is relatively large, all of the flash-mixed tracks produced by such flash mixing fall within a narrow temperature range. The offset in luminosity among these tracks is due to small differences in the helium-core mass. As can be seen in Figure 3, flash-mixed models can reproduce the faint luminosities observed in the BH population, particularly the flash-mixed models originating in a subpopulation with enhanced helium.

There is one obvious problem, however. Flash-mixed models (whether originating in a population with enhanced or standard Y) cannot reproduce the reddest stars in the BH population. Brown et al. (2001) explored various ways of producing such red subluminous stars, including enhanced line blanketing in the atmosphere, due to an increase in the atmospheric iron abundance via radiative diffusion. This explanation is explored in more detail in the next section, where we obtained spectroscopy of two of these curiously red BH stars.

The BH phenomenon appears to be restricted to the most massive globular clusters in the Galaxy (Brown et al. 2010, and references therein). Of the clusters that have extended HBs and UV imaging, only those clusters with masses exceeding 1.2×10^6 $M_\odot$ exhibit BH stars. This is not because massive clusters offer more stellar mass for finding rare objects. If one constructs a virtual globular cluster by summing all of the known low-mass clusters that have extended HBs and UV imaging, this virtual cluster would have a mass of 5.1×10^6 $M_\odot$ (exceeding any known globular cluster), yet it would host only a few BH stars; we would expect dozens of such stars if we were to scale from the numbers of BH stars present in actual massive clusters. One can also see the importance of cluster mass by comparing the UV CMDs of individual clusters hosting similar numbers of EHB stars. For example, the published CMDs of NGC 6752 (Landsman et al. 1996, $M \approx 3\times10^5$ $M_\odot$) and NGC 2808 (Brown et al. 2001, $M \approx 3\times10^6$ $M_\odot$) each include approximately 80 EHB stars, but all of the EHB stars in NGC 6752 are normal, while half of the EHB stars in NGC 2808 are subluminous (i.e., BH stars). Because a delayed core flash is more likely in stars that were born with an enhanced helium abundance ($Y \sim 0.4$), BH stars may only form in those clusters massive enough to retain the helium-rich ejecta from the first stellar generation of stars,

3. Spectroscopy

Spectroscopic evidence for flash mixing includes *Far Ultraviolet Spectroscopic Explorer (FUSE)* observations of field stars, Very Large Telescope (VLT) observations of

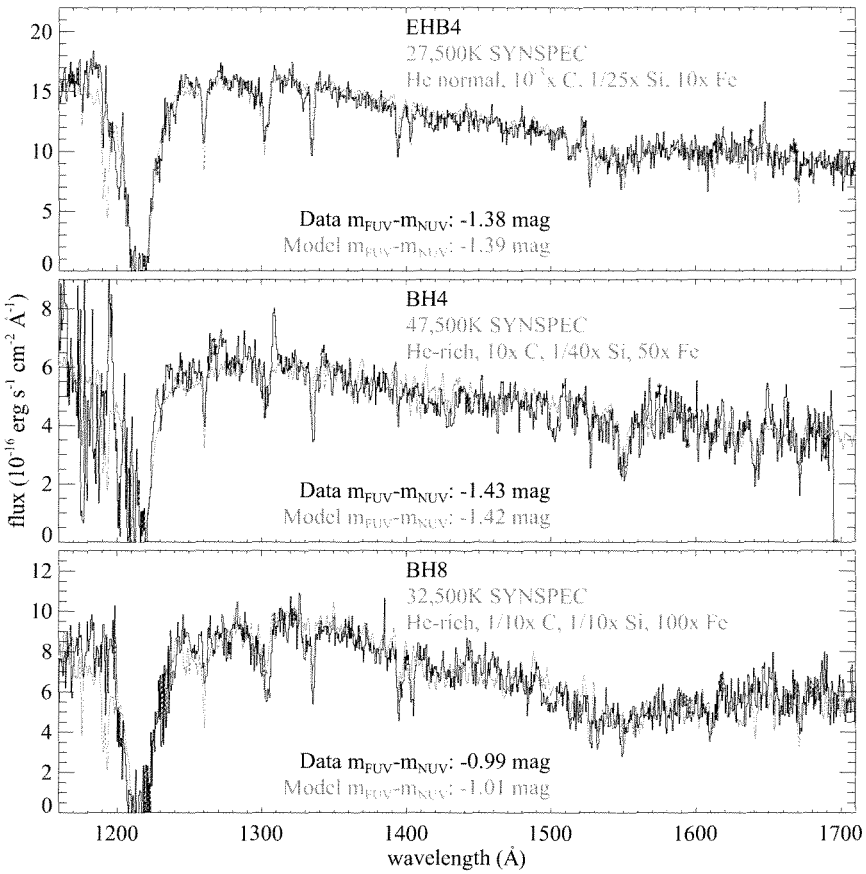

Figure 4. Representative spectra from our sample: a normal EHB star (*top panel*), a BH star (*middle panel*), and one of the unusually red subluminous stars (*bottom panel*). In each panel, we also show a synthetic spectrum (grey curve) that matches both the observed spectrum (Brown et al. 2011) and UV photometry (Brown et al. 2001). Compared to the normal EHB stars, the BH stars are hotter and have stronger helium and carbon lines, as expected if the BH stars formed via flash mixing. The BH stars all exhibit enhanced iron-peak abundances, while the normal EHB stars are mixed, with some enhanced and others not. Some subluminous EHB stars are much redder than expected (see Figure 3), but their red colors can be explained by a large enhancement of iron-peak elements, presumably from radiative levitation.

EHB stars in ω Cen, and *HST*/STIS observations of both normal and subluminous EHB stars in NGC 2808.

In the Galactic field population, sdB stars are the analogs to the EHB stars found in globular clusters. Because the helium-rich sdB stars (He-sdB stars) seemed to be the most likely candidates for flash mixing in the field population, Lanz et al. (2004) obtained *FUSE* spectroscopy of three He-sdB stars to characterize their helium, carbon, and nitrogen abundances. Two of these stars (PG1544+488 and JL87) exhibit enormous carbon enhancements, in excellent agreement with the expectations from flash mixing.

Specifically, PG1544+488 has a surface composition of 96% helium, 2% carbon, and 1% nitrogen, while JL87 has a similar composition (although it retains more surface hydrogen). The spectra of these two stars are among the strangest in the *FUSE* archive, with carbon lines stronger than the Lyman series.

ω Cen is the most massive globular cluster in the Galaxy, and the cluster where UV photometry first revealed the existence of BH stars (D'Cruz et al. 1996, 2000). Using optical photometry of the cluster, Moehler et al. (2011) selected the faintest and hottest EHB stars in ω Cen to produce a sample that was likely to include BH stars, although these stars did not have the UV photometry required to demonstrate that any particular star is subluminous. They obtained FLAMES+GIRAFFE spectroscopy on the VLT over the spectral range of 3964–4567 Å for 109 EHB stars. They found that the stars at $T_{\rm eff}$ <30,000 K are helium-poor, but that nearly three quarters of the stars at hotter temperatures have solar or enhanced helium abundance. They also found the carbon abundance to be strongly correlated with the helium abundance, with carbon approaching ~3% by mass.

In late 2010 and early 2011, we obtained *HST*/STIS spectroscopy of 24 hot stars in NGC 2808, drawn from its UV CMD (Brown et al. 2001, Figure 3). This sample includes 7 normal EHB stars and 8 BH stars. It also includes 5 cooler stars on the blue HB, a post-EHB star, and three unclassified objects significantly hotter than the canonical EHB. Here we restrict the discussion to the 15 EHB and BH stars (for the full sample, see Brown et al. 2011).

Figure 4 shows representative spectra from our sample. For comparison, we show a non-LTE synthetic spectrum that matches the far-UV spectroscopy (Brown et al. 2011) and UV photometry (Brown et al. 2001). To ease interpretation, the abundances of carbon, silicon, and iron are specified relative to the mean cluster abundance, which we assume to be [Fe/H]= −1.36 with [α/Fe]=0.3. Our "helium normal" models assume Y = 0.23 while our "helium rich" models assume Y = 0.99. Figure 5 shows the composite spectrum of all normal EHB stars in our sample compared to the composite spectrum of all BH stars in our sample. The BH stars are much hotter than the normal EHB stars, and they exhibit much stronger carbon and helium features, as expected if the BH stars formed via flash mixing. The silicon lines vary significantly from star to star, presumably due to atmospheric diffusion, but on average the normal EHB stars and the BH stars have similar silicon abundances. Two of our BH stars fall in the temperature range (48,000 K $\lesssim T_{\rm eff} \lesssim$ 52,000 K) spanned by pulsating subdwarfs recently discovered in ω Cen (Randall et al. 2011). Randall et al. (2011) suggest this is a new instability strip, and so our hottest BH stars may also be pulsators. Such an instability strip would be better populated in massive globular clusters than in the Galactic field population; massive clusters host subpopulations enhanced in helium ($Y \sim 0.4$), and such populations are more likely to produce hotter subdwarfs through flash mixing.

All of the BH stars exhibit enhanced iron-peak abundances, while the normal EHB stars are mixed, with some exhibiting normal iron-peak abundances and others showing enhancement. The distortion of the normal abundance pattern by atmospheric diffusion in hot subdwarfs is well documented (e.g., Heber 2009), although other processes, such as turbulent mixing and mass loss, also play a role in these anomalies (Hu et al. 2011). The two reddest stars in our BH sample exhibit deep and broad absorption troughs from the iron-peak elements (Figure 4). Subluminous EHB stars with such red colors have been difficult to explain (Brown et al. 2010, Figure 3), but our spectra indicate that they may be extreme cases of metal enhancement through radiative levitation.

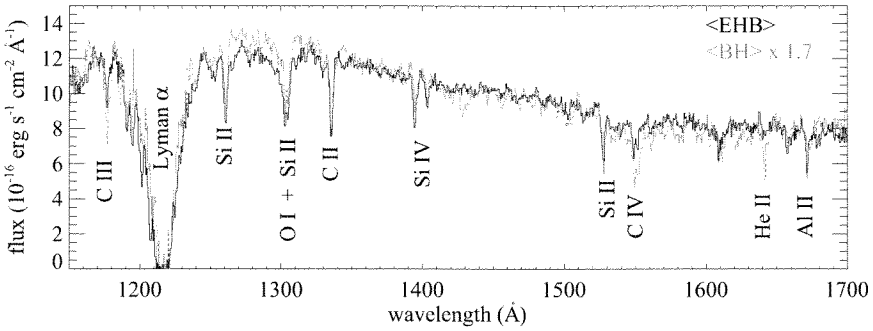

Figure 5. The composite spectrum for all normal EHB stars in our sample (black curve) compared to the composite spectrum for all BH stars in our sample (grey curve). The Si II, O I, C II, and All II lines are all interstellar. Si IV and C IV have both an interstellar component and a photospheric component. C III and He II are purely photospheric. The BH spectrum has stronger carbon and helium absorption, as expected from flash mixing.

The fact that the BH stars show much stronger helium and carbon lines, when compared to the normal EHB stars, is qualitatively in line with expectations from flash mixing. However, in the BH sample, the carbon abundance is not as high as one would expect for a star that recently emerged from flash mixing. In a flash-mixed star, carbon (and/or nitrogen) should comprise up to 4% of the atmosphere by mass (see, for example, Lanz et al. 2004). In contrast, the strongest carbon enhancement found in our BH sample corresponds to a carbon abundance that is 0.2% by mass. Furthermore, the carbon abundance in the normal EHB sample is strongly reduced with respect to the mean abundance in the cluster, and is orders of magnitude smaller than in the BH stars. It appears that both the normal EHB sample and the BH sample suffer from depleted carbon abundances. This is not unexpected. The numerical simulations of Miller Bertolami et al. (2008) trace the atmospheric abundances of stars as they evolve through the flash mixing stage and into the subsequent period of stable core helium burning, accounting for atmospheric diffusion due to gravitational settling and radiative levitation. They found that the carbon abundance declines rapidly after a star emerges from the flash-mixing process, dropping by an order of magnitude after 1000 years, and by several orders of magnitude 10^7 years later. The star spends only a small fraction of its stable core helium-burning lifetime with a carbon abundance near its maximum of ~1–4% by mass. The diffusion models indicate that the helium abundance will also decline with time. However, these results assume that atmospheric diffusion is not inhibited by such processes as mass loss, turbulence, and surface convection.

4. Summary

Although blue hook stars are rare, they have a significant presence in the UV CMDs of massive globular clusters. Such clusters also possess complex optical CMDs, which exhibit splitting of the main sequence and subgiant branch, indicating the presence of subpopulations enhanced in helium ($Y \sim 0.4$; Piotto et al. 2005). Although stars born with enhanced helium ($Y \sim 0.4$) are more likely to become EHB stars, we have shown

that only flash mixing leads to the luminosity range needed to produce the blue hook feature in the UV CMDs of massive globular clusters. For those stars suffering high mass loss on the RGB, the helium-core flash will be delayed to the WD cooling curve. The flash mixing of the envelope associated with such a delayed helium-core flash will produce hotter EHB stars that are enhanced in atmospheric helium and carbon, relative to their normal EHB brethren. The larger bolometric correction and reduced opacity below the Lyman limit in the flash-mixed stars makes them appear subluminous in the UV and optical. Our UV spectroscopy of both normal and subluminous EHB stars in one such cluster (NGC 2808) demonstrates that the blue hook population is hotter than the normal EHB population, even though the normal and subluminous EHB samples span similar ranges in UV color. Moreover, the blue hook stars exhibit much stronger absorption lines of carbon and helium, as expected from flash mixing. It is also clear that both the EHB and BH samples have abundance patterns that have been altered by atmospheric diffusion. The reddest of the subluminous EHB stars may be explained by radiative levitation of the iron-peak elements in the atmospheres of these stars.

Acknowledgments. Support for programs 10815 and 11665 are provided through a NASA grant from STScI, which is operated by AURA under contract NAS 5-26555.

References

Brown, T.M., Lanz, T., Sweigart, A.V., Cracraft, M., & Hubeny, I. 2011, ApJ, submitted
Brown, T.M., Sweigart, A.V., Lanz, T., Landsman, W.B., & Hubeny, I. 2001, ApJ, 562, 368
Brown, T.M., Sweigart, A.V., Lanz, T., Smith, E., Landsman, W.B., & Hubeny, I. 2010, ApJ, 718, 1332.
Busso, G., et al. 2007, A&A, 474, 105
Castellani, M., & Castellani, V. 1993, ApJ, 407, 649
D'Antona, F., Bellazzini, M., Caloi, V., Pecci, F.F., Galleti, S., & Rood, R.T. 2005, ApJ, 631, 868
D'Cruz, N.L., Dorman, B., Rood, R.T., & O'Connell, R.W. 1996, ApJ, 466, 359
D'Cruz, N.L., O'Connell, R.W., Rood, R.T., Whitney, J.H., Dorman, B., Landsman, W.B., Hill, R.S., Stecher, T.P., & Bohlin, R.C. 2000, ApJ, 530, 352
Dieball, A., Knigge, C., Maccarone, T.J., Long, K.S., Hannikainen, D.C., Zurek, D., & Shara, M. 2009, MNRAS, 394, L56
Heber, U. 2009, ARAA, 47, 211
Hu, H., Tout, C.A., Glebbeek, E., & Dupret, M.-A. 2011, MNRAS, in press.
Landsman, W.B., Sweigart, A.V., Bohlin, R.C., Neff, S.G., O'Connell, R.W., Roberts, M.S., Smith, A.M., & Stecher, T.P. 1996, ApJ, 472, L93
Lanz, T., Brown, T.M., Sweigart, A.V., Hubeny, I., & Landsman, W.B. 2004, ApJ, 602, 342
Layden, A.C., & Sarajedini, A. 2000, AJ, 119, 1760
Miller Bertolami, M.M., Althaus, L.G., Unglaub, K., & Weiss, A. 2008, A&A, 491, 253.
Moehler, S., Dreizler, S., Lanz, T., Bono, G., Sweigart, A.V., Calamida, A., & Nonino, M. 2011, A&A, 526, A136
Piotto, G., Bedin, L.R., Anderson, J., King, I.R., Cassisi, S., Milone, A.P., Villanova, S., Pietrinferni, A., & Renzini, A. 2007, ApJ, 661, L53
Piotto, G., et al. 2005, ApJ, 621, 777
Piotto, G., Zoccali, M., King, I.R., Djorgovski, S.G., Sosin, C., Rich, R.M., & Meylan, G. 1999, ApJ, 118, 1727
Randall, S.K., Calamida, A., Fontaine, G., Bono, G., & Brassard, P. 2011, ApJ, 737, L27
Ripepi, V., et al. 2007, ApJ, 667, L61
Rich, R.M., et al. 1997, ApJ, 474, L25
Rosenberg, A., Recio-Blanco, A., García-Marín, M. 2004 ApJ, 603, 135
Siegel, M.H., et al. 2007, ApJ, 667, L57